Conditional knockin of Dnmt3a R878H initiates acute myeloid leukemia with mTOR pathway involvement

Yu-Jun Dai[a,1], Yue-Ying Wang[a,1,2], Jin-Yan Huang[a,1], Li Xia[a,1], Xiao-Dong Shi[a], Jie Xu[a], Jing Lu[a], Xian-Bin Su[b], Ying Yang[a], Wei-Na Zhang[a], Pan-Pan Wang[a], Song-Fang Wu[a], Ting Huang[a], Jian-Qing Mi[a], Ze-Guang Han[b], Zhu Chen[a,b,2], and Sai-Juan Chen[a,b,2]

[a]State Key Laboratory of Medical Genomics, Shanghai Institute of Hematology, Rui Jin Hospital, Shanghai Jiao Tong University School of Medicine, Shanghai 200025, China; and [b]Key Laboratory of Systems Biomedicine, Ministry of Education, Shanghai Center for Systems Biomedicine, Shanghai Jiao Tong University, Shanghai 200240, China

Contributed by Zhu Chen, April 2, 2017 (sent for review March 3, 2017; reviewed by Tao Cheng and Margaret A. Goodell)

***DNMT3A* is frequently mutated in acute myeloid leukemia (AML). To explore the features of human AML with the hotspot *DNMT3A* R882H mutation, we generated Dnmt3a R878H conditional knockin mice, which developed AML with enlarged $Lin^{-}Sca1^{+}cKit^{+}$ cell compartments. The transcriptome and DNA methylation profiling of bulk leukemic cells and the single-cell RNA sequencing of leukemic stem/progenitor cells revealed significant changes in gene expression and epigenetic regulatory patterns that cause differentiation arrest and growth advantage. Consistent with leukemic cell accumulation in G_2/M phase, CDK1 was up-regulated due to *mTOR* activation associated with DNA hypomethylation. Overexpressed CDK1-mediated EZH2 phosphorylation resulted in an abnormal trimethylation of H3K27 profile. The mTOR inhibitor rapamycin elicited a significant therapeutic response in $Dnmt3a^{R878H/WT}$ mice.**

Dnmt3a R878H mutation | conditional knockin mice | single-cell RNA-seq | leukemia | mTOR inhibitor

Somatic mutations in the DNA methyltransferase *DNMT3A* have been identified in a subset of acute myeloid leukemia (AML), myelodysplastic syndrome (MDS), and acute lymphoblastic leukemia (ALL), with DNMT3A R882 being the hotspot (1–4). Clinical features of most AML cases with *DNMT3A* mutations include preferential involvement of a monocytic lineage (AML-M4 and -M5 subtypes), thrombocytosis, onset at a relatively old age, and poor prognosis (2, 5, 6). Careful genotype–phenotype correlations suggest that patients manifest *DNMT3A* mutations in preleukemic hematopoietic stem cells (HSCs)/multipotent progenitors (MPPs), which exhibit a competitive advantage over normal HSCs. Because these mutations occur at a very early stage among genetic abnormalities, they are likely involved in the development of leukemia (7, 8).

Functionally, the DNMT3A R882 mutation might disrupt epigenetic regulation. This kind of *DNMT3A* mutation confers reduced methyltransferase activity and promotes the possibility of dominant-negative consequences compared with the wild-type (WT) allele (2, 9, 10). Moreover, the *DNMT3A* mutation causes aberrant DNA hypomethylation and up-regulates a series of target genes involved in AML pathogenesis (11–13).

In vivo animal tests have shown that the *Dnmt3a* gene plays an essential role in hematopoiesis regulation. $Dnmt3a^{-/-}$ HSCs expand remarkably, but their differentiation is inhibited when *Dnmt3a* is conditionally inactivated in the murine hematopoietic system; this phenomenon is consistent with a preleukemic state (7). Moreover, all lethally irradiated mice transplanted with *Dnmt3a*-deleted HSCs died within 1 y and were diagnosed with a spectrum of malignancies similar to those observed in patients carrying *DNMT3A* mutations, including MDS, AML, primary myelofibrosis, and ALL, suggesting that Dnmt3a functions as a tumor suppressor (7). With a second hit of mutations in various genes such as *N-RAS*, *C-KIT*, or *FLT3* in $Dnmt3a^{-/-}$ mice, *Dnmt3a* deletion induces leukemic transformation (14, 15). Although these results indicate a major role of *Dnmt3a* deletion in facilitating the development of leukemia, the in vivo roles of DNMT3A mutants in leukemogenesis still need to be addressed. In our previous work, bone marrow transplantation (BMT) of bone marrow (BM) cells retrovirally transduced with DNMT3A R882H induced chronic myelomonocytic leukemia (CMML) with mild invasive behaviors through disturbing DNA methylation and gene expression in recipient mice (12). In contrast to the aggressive manifestations of *DNMT3A* mutation-related AML in clinical settings, this phenotype can be ascribed to an inappropriate expression of the mutant *DNMT3A* gene as driven by a retroviral promoter instead of the endogenous promoter/enhancer.

To address whether the clinically significant *DNMT3A* mutation could really be leukemogenic, we established a conditional knockin mouse model and investigated genetic and epigenetic changes, including gene expression profiles, DNA methylation, and chromatin modification, affected by this mutation. We further explored the potential mechanisms that can explain the process by which the *DNMT3A* mutation hierarchically induces abnormal hematopoiesis and the manner by which specific regulators of relevant pathways in murine and human settings can be targeted for potential therapeutic applications.

Significance

DNMT3A is a critical epigenetic modifier and tumor suppressor in the hematopoietic system. This gene is frequently mutated in hematopoietic malignancies, including acute myeloid leukemia (AML), with Dnmt3a R878H being the most common mutant. By using a conditional knockin approach, this study shows that Dnmt3a R878H is sufficient to initiate AML and recapitulate human leukemic features in mice. The leukemia-initiating cells are enriched in hematopoietic stem/progenitor cells. Through gene expression profiling, DNA methylation and histone modification analysis, and functional tests on important regulators for cell proliferation and differentiation in an animal model, this study has not only discovered mTOR pathway activation as a key player in the disease mechanism but also revealed the potential therapeutic effects of mTOR inhibition on *DNMT3A* mutation-related leukemia.

Author contributions: Y.-Y.W., Z.C., and S.-J.C. designed research; Y.-J.D., Y.-Y.W., L.X., X.-D.S., J.X., J.L., X.-B.S., Y.Y., W.-N.Z., P.-P.W., S.-F.W., T.H., J.-Q.M., and Z.-G.H. performed research; J.-Y.H. contributed to bioinformatics analysis; Y.-J.D., Y.-Y.W., Z.C., and S.-J.C. analyzed data; and Y.-J.D., Y.-Y.W., Z.C., and S.-J.C. wrote the paper.

Reviewers: T.C., Chinese Academy of Medical Sciences and Peking Union Medical College; and M.A.G., Baylor College of Medicine.

The authors declare no conflict of interest.

[1]Y.-J.D., Y.-Y.W., J.-Y.H., and L.X. contributed equally to this work.

[2]To whom correspondence may be addressed. Email: wyymoon@hotmail.com, zchen@stn.sh.cn, or sjchen@stn.sh.cn.

This article contains supporting information online at www.pnas.org/lookup/suppl/doi:10.1073/pnas.1703476114/-/DCSupplemental.

Results

***Dnmt3a* R878H Mutation Induces AML in Conditional Knockin Mice.** To elucidate the consequences of the DNMT3A R882 mutant in an endogenous expression environment, we generated a mouse model of Cre-mediated conditional expression of mutant Dnmt3a R878H obtained from the endogenous locus of *Dnmt3a* (Fig. S1*A*). Dnmt3a R878H knockin mice were crossed with mice carrying a Cre recombinase allele under the control of an IFN-inducible Mx1 promoter (Mx1Cre). Upon Cre induction with pIpC, the endogenous *Dnmt3a* exon 23 was efficiently replaced by exon 23 carrying the R878H mutation in the hematopoietic system, whereas this replacement was not found in other organs/tissues examined (Dataset S1). Conditional *Dnmt3a* R878H expression and activation were directed to the hematopoietic compartment by the Mx1 promoter. After obtaining Mx1Cre^{+}Dnmt3a$^{R878H/WT}$ heterozygous mice (Dnmt3a$^{R878H/WT}$), we confirmed the genotype at the DNA level and checked the RNA expression of the mutation by using PCR and sequence analysis (Fig. S1*B*).

Approximately 4 to 6 mo after IFN induction, all 25 Dnmt3a$^{R878H/WT}$ mice were diagnosed with a myelomonocytic type of AML characterized by segmental expansion of immature cells in the BM and spleen, along with extramedullary infiltration (splenomegaly, lymphadenectasis, and cutaneous invasion). The Dnmt3a$^{R878H/WT}$ mice showed a relatively long median survival time of 230 d (Fig. 1*A*). Large leukemic cells showing a high nuclear/cytoplasmic ratio and fine chromatin were observed in the BM (23% on average) and spleen of all Dnmt3a$^{R878H/WT}$ mice (Fig. 1*C*). The nuclei of some blasts were indented, reminiscent of the identity of monoblasts (Fig. 1*B*). The inhibition ratio of NaF in BM cells was higher than 50%, indicating that these immature cells belonged to the monocytic lineage. Peripheral blood (PB) analysis showed significantly increased numbers of white blood cells (WBCs) and platelets and a dramatically reduced hemoglobin level (Fig. S1*C*). PB smears with Wright's staining revealed a striking feature: a significant amount of early myeloid elements against a background of increased granulocytes, monocytes, and clustered platelets (Fig. S1*D*). In addition, the Dnmt3a$^{R878H/WT}$ mice displayed a reduced number of lymphocytes in the BM compared with those in Dnmt3a$^{WT/WT}$ controls (Fig. 1*C*). To determine whether cooperating mutations occurred in Dnmt3a$^{R878H/WT}$ leukemic mice, we performed whole-exome sequencing (WES) in BM samples and paired normal tail specimens from three diseased animals. We identified 17 potential somatic sequence changes in the coding region, including 16 single-nucleotide variations (SNVs) and 1 small deletion (Dataset S2). However, none of the SNVs was recurrent or previously reported in leukemia-related genes. Our data suggested that the Dnmt3a R878H mutant might be a driver of leukemogenesis.

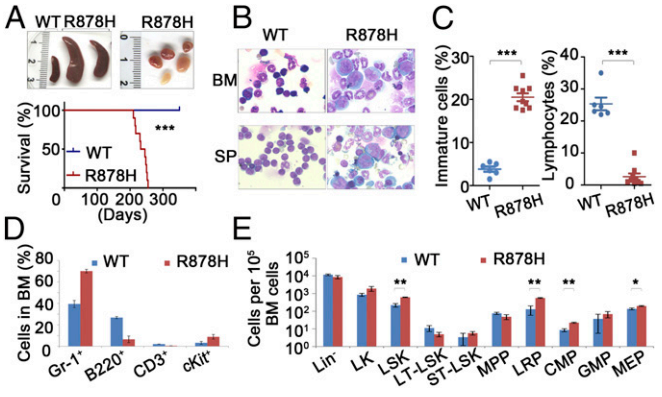

Fig. 1. Dnmt3a$^{R878H/WT}$ mice develop AML characterized by expansion of HSPCs. (*A*, *Upper*) Macroscopic appearance of spleen and lymphoid nodes obtained from mice. No lymphadenopathy was observed in WT animals. (*Lower*) Kaplan–Meier survival curves of Dnmt3a$^{WT/WT}$ (n = 15) and Dnmt3a$^{R878H/WT}$ (n = 10) mice. (*B*) Morphological analysis of BM and spleen (SP) obtained from mice. Wright's staining was performed on BM and SP cytospin preparations. (*C*) Statistical analysis of the number of immature cells and lymphocytes in the BM. (*D* and *E*) Flow cytometric quantification of mature hematopoietic cell populations and the indicated HSPC populations in BM cells of mice. Mean ± SEM values are shown. *P < 0.05, **P < 0.01, ***P < 0.001.

Hematopoietic Progenitors Are Significantly Increased in Dnmt3a$^{R878H/WT}$ Mice. In view of the significant myelomonocytosis in leukemic mice, we hypothesized that lineage-restricted progenitors (LRPs) and common myeloid progenitors (CMPs) should be affected. To further explore the unique AML phenotype induced by Dnmt3a R878H, we traced emerging hematopoietic stem/progenitor cell (HSPC) compartments for precise analysis. Flow cytometric analyses revealed an altered granulocyte/lymphocyte ratio and increased cKit^{+} cells in the BM, spleen, and PB of Dnmt3a$^{R878H/WT}$ mice (Fig. 1*D* and Fig. S1 *E*–*H*). Interestingly, the lineage-negative (Lin^{-}) cells were significantly expanded in the BM, along with the majority of leukemic cells appearing in the Gr-1^{+} compartment. Lin^{-}Sca1^{+}cKit^{+} (LSK) cells were increased by ∼3- to 10-fold. The LSK population contains long-term HSCs (LT-HSCs), short-term HSCs (ST-HSCs), MPPs, and LRPs (16). We found that among the LSK cells the number of LT-HSCs decreased, quantity of ST-HSCs remained unchanged, and LRPs remarkably expanded from 70% up to 90% of LSKs in Dnmt3a$^{R878H/WT}$ mice. Moreover, the LK (Lin-Sca1-cKit^{+}) population containing CMPs, granulocyte-macrophage progenitors (GMPs), and megakaryocyte-erythroid progenitors (MEPs) were investigated. Leukemic mice demonstrated an increase in CMPs and MEPs but not GMPs (Fig. 1*E* and Fig. S1*I*).

LSK Cells from Dnmt3a$^{R878H/WT}$ Mice Harbor Leukemia-Initiating Cells. Because the LSK compartment was considerably enlarged in leukemic BM, we hypothesized that the aberrantly increased LSK cells might contain leukemia-initiating cells. Therefore, the effect of *Dnmt3a* R878H on leukemogenesis was further investigated through transplantation experiments by inoculating 1,000 LSK cells derived from the BM of Dnmt3a$^{WT/WT}$ or diseased Dnmt3a$^{R878H/WT}$ donor mice (with the CD45.2 marker) into sublethally irradiated (350 cGy) recipient mice (with the CD45.1 marker). As shown in Fig. 2*A*, almost no CD45.2-expressing elements were detectable in the PB of mice receiving Dnmt3a$^{WT/WT}$ LSK cells during the 9 mo after transplantation. In contrast, the percentage of CD45.2^{+} WBCs in the PB increased significantly to a level of 53% in recipient mice with a Dnmt3a$^{R878H/WT}$ transplant over the same period, suggesting that *Dnmt3a* R878H might provide LSK cells with an advantage in growth and survival. Detailed phenotype analysis was performed in three of the mice inoculated with Dnmt3a$^{R878H/WT}$ LSK cells. Similar to the observation in primary Dnmt3a$^{R878H/WT}$ animals, these mice manifested a high WBC count of up to 30 × 10^{9}/L, high numbers of platelets and a reduced hemoglobin level (Fig. 2*B* and Fig. S2*A*), an average of 20% immature cells in the BM, splenomegaly, and lymphadenectasis (Fig. 2*C*). These results indicated that the leukemia induced by knockin of Dnmt3a R878H was transplantable and that the LSK cells with the *Dnmt3a* mutation might harbor leukemia-initiating cells. Moreover, we also transplanted 2 × 10^{6} spleen cells from the Dnmt3a$^{R878H/WT}$ leukemic mice into secondary recipient mice, which developed AML with a longer latency (12 to 18 mo) compared with the experiment using leukemic LSK cells.

Single-Cell Transcriptome Profiling of LSKs in Dnmt3a$^{R878H/WT}$ Leukemic Mice. To obtain insight into the biological signature of leukemic progenitors, we compared gene expression profiles of LSKs between Dnmt3a$^{WT/WT}$ and Dnmt3a$^{R878H/WT}$ mice by using single-cell RNA sequencing (RNA-seq) (Fig. S2*B*). The possible differences in heterogeneity of gene expression in terms of functional categories between Dnmt3a$^{WT/WT}$ and Dnmt3a$^{R878H/WT}$

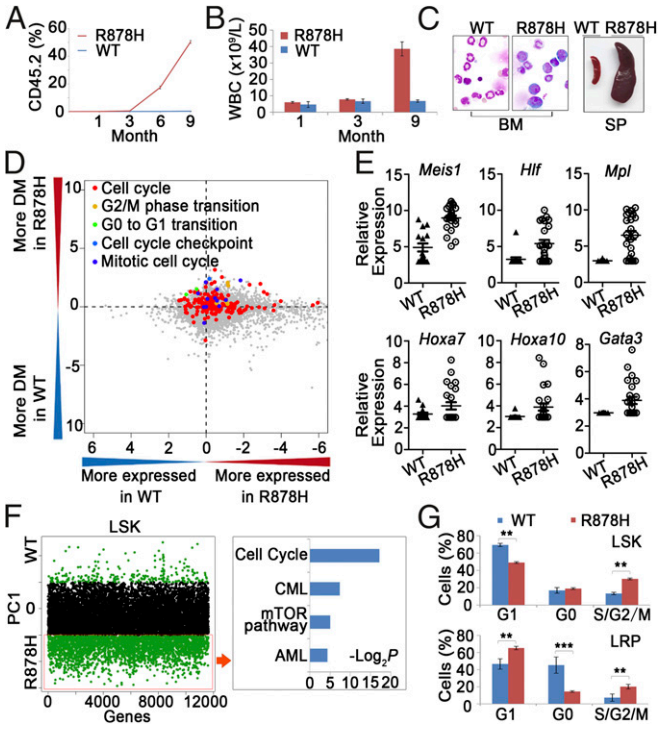

Fig. 2. Functional analysis of LSKs and single-cell transcriptome profiling of LSKs. (*A*) The percentage of CD45.2$^+$ cells in the PB of recipient mice (CD45.1$^+$ marker) after transplantation of LSKs. (*B*) Statistical analysis of cell counts in the PB after transplantation of LSKs. (*C*) Morphological analysis of BM and SP obtained from the LSK-transplanted mice. (*D*) Comparison between LSKs from Dnmt3a$^{WT/WT}$ and Dnmt3a$^{R878H/WT}$ mice in terms of their levels of gene expression and heterogeneity for GO categories. The logarithm (log10) of *P* values from two-sided paired *t* tests applied to mean normalized read counts (*x* axis) and DMs (*y* axis) was computed for each GO category and plotted against each other by multiplying the sign of the *t* statistic. (*E*) Expression level of genes associated with hematopoietic differentiation and leukemogenesis in LSKs. (*F*, *Left*) Distribution of genes contributing to principal component 1 (PC1) separation based on PCA. Green dots above and below the black dot zone represent down-regulated and up-regulated genes, respectively. (*Right*) Identification of leukemogenesis-related pathways based on KEGG enrichment analysis. (*G*) Flow cytometric analyses for the cell cycle of the indicated LSKs and LRPs. Mean ± SEM values are shown. $^{**}P < 0.01$, $^{***}P < 0.001$.

mice were further investigated (Dataset S3): We compared distance-to-the-median (DM) values of genes in mouse pairs for each Gene Ontology (GO term) as previously described (17). Altogether, 1,039 GO terms revealed significant differences in at least one pairwise comparison ($P < 0.01$) (Dataset S4). The expression of genes involved in cell-cycle regulation and transition were more heterogeneous in Dnmt3a$^{R878H/WT}$ mice than in Dnmt3a$^{WT/WT}$ ones (Fig. 2*D*). Some genes associated with leukemogenesis, such as *Meis1*, *Hlf*, *Mpl*, *Hoxa7*, *Hoxa10*, and *Gata3* were up-regulated in LSKs of Dnmt3a$^{R878H/WT}$ mice (Fig. 2*E*). Principal component analysis (PCA) of the transcriptome demonstrated a separated LSK cluster, except for one sample, of Dnmt3a$^{R878H/WT}$ from LSKs derived from Dnmt3a$^{WT/WT}$ animals, revealing that most LSKs in diseased mice displayed distinct transcriptome identities. We then combined RNA-seq data of all the individual LSKs into Dnmt3a$^{WT/WT}$ and Dnmt3a$^{R878H/WT}$ groups to access their global expression profiles. Kyoto Encyclopedia of Genes and Genomes (KEGG) enrichment analysis (Dataset S5) showed that genes involved in the cell-cycle, chronic myeloid leukemia (CML), mTOR, and AML signaling pathways were overexpressed and responsible for the separation of leukemic and Dnmt3a$^{WT/WT}$ LSK clusters (Fig. 2*F*). These results were consistent with the cell-cycle status of LSKs as determined by flow cytometric analysis showing the transition of G_0/G_1 to $S/G_2/M$ (Fig. 2*G* and Fig. S2*C*). In fact, many cell-cycle regulators, such as cyclin-dependent kinase (CDK) family genes (including *Cdk11b*, *Cdk6*, *Cdkn1a*, and *Cdk20*), which are involved in this transition and presumably cause cell proliferation, were overexpressed (Dataset S3).

Transcriptome Profiling of Gr-1$^+$ Leukemic Cells in Dnmt3a$^{R878H/WT}$ Mice. The majority of leukemic cells in Dnmt3a$^{R878H/WT}$ mice were Gr-1$^+$ cells, which could originate from the LSK population. Therefore, it is reasonable to hypothesize that Gr-1$^+$ leukemic cells might possess migratory and invasive capacities resulting in the unique disease phenotype. To further address the mechanism underlying leukemogenesis, we performed transcriptome profiling through RNA-seq of Gr-1$^+$ leukemic cells (Dataset S6). The *Dnmt3a* R878H allele was transcriptionally expressed. Gene set enrichment analysis (GSEA) showed a statistically significant enrichment of the cell-cycle pathway in the Gr-1$^+$ cells of Dnmt3a$^{R878H/WT}$ mice compared with Dnmt3a$^{WT/WT}$ mice. By contrast, the enrichment of the mature hematopoietic cell-lineage pathway was prominent in Gr-1$^+$ cells of Dnmt3a$^{WT/WT}$ mice (Fig. 3*A*). At individual gene levels, many genes associated with proliferation, such as *Pcna* and *Cdk* family members (*Cdk1*

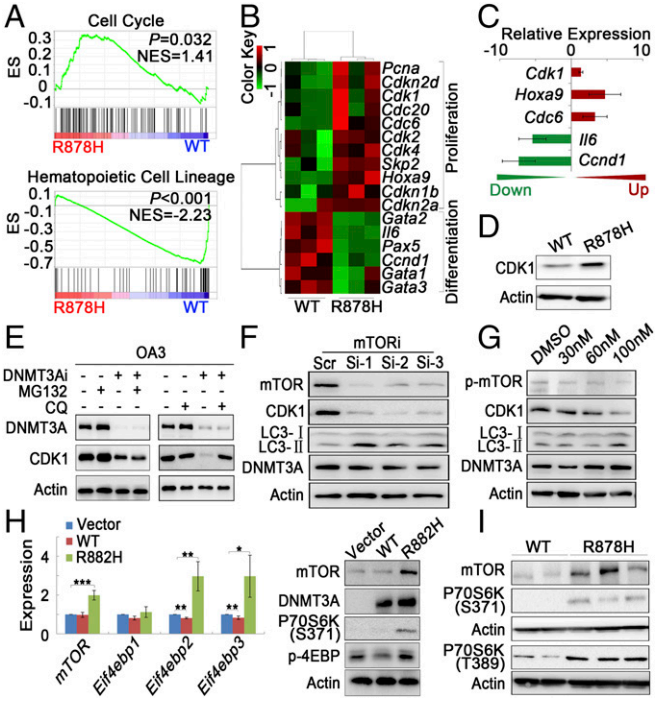

Fig. 3. Transcriptome profiling of Gr-1$^+$ leukemic cells and mTOR-mediated CDK1 overexpression induced by Dnmt3a mutation. (*A*) GSEA analysis of differentially expressed genes in Gr-1$^+$ cells. NES, normalized enrichment score. (*B*) Heatmap of hematopoietic cell proliferation- and differentiation-related genes that are differentially expressed in Dnmt3a$^{WT/WT}$ and Dnmt3a$^{R878H/WT}$ mice. Red and green colors indicate up-regulated and down-regulated genes, respectively. (*C*) Gene expression levels were validated by RT-PCR. (*D*) Lysates from BM cells of mice were analyzed by Western blot with the indicated antibodies. (*E*) OA3 cells transfected with scrambled (DNMT3Ai–) or DNMT3A siRNA (DNMT3Ai+) were treated with MG132 or CQ, and their lysates were analyzed with Western blot. (*F* and *G*) Lysates from OA3 cells transfected with three siRNAs (1 to 3) against different *mTOR* regions or treated with different doses of rapamycin were analyzed with Western blot. (*H*) Results of RT-PCR and Western blot analysis for mTOR and its downstream genes in NIH 3T3 cells transfected with vehicle, WT, or R882H DNMT3A. (*I*) Lysates from BM cells of mice were analyzed with Western blot. Mean ± SEM values are shown. $^{*}P < 0.05$, $^{**}P < 0.01$, $^{***}P < 0.001$.

and *Cdk2*), were overexpressed in Gr-1$^+$ cells, which was consistent with the results in the LSKs of Dnmt3a$^{R878H/WT}$ mice. However, a number of hematopoietic differentiation-related genes, such as *Gata1* to *3* and *Pax5*, were expressed at a low level in the Gr-1$^+$ cells of Dnmt3a$^{R878H/WT}$ mice (Fig. 3*B*). A portion of the differentially expressed genes were confirmed by real-time RT-PCR (Fig. 3*C*).

***Dnmt3a* Mutation Increases CDK1 Protein Level Through mTOR Activation.** To further explore the mechanism underlying Dnmt3a$^{R878H/WT}$ phenotypic defects, we also tried to identify abnormal regulatory networks through protein-level analysis. To this end, CDK1 overexpression was discovered while screening proteins associated with the cell cycle in BM cells of Dnmt3a$^{R878H/WT}$ mice compared with Dnmt3a$^{WT/WT}$ animals (Fig. 3*D*). To facilitate detailed biochemical and molecular studies and ultimately clarify the mechanism by which the *DNMT3A* mutation induces CDK1 up-regulation, we used two cell models, the human cell line OCI-AML3 (OA3) harboring the DNMT3A R882C mutation and the murine fibroblast line NIH 3T3 stably expressing DNMT3A R882H. Knockdown of mutant protein expression with RNAi substantially decreased CDK1 protein, but not its mRNA, in OA3 cells, suggesting that the DNMT3A R882 mutation could affect the turnover of CDK1 protein (Fig. S3*A*). Furthermore, we applied the lysosome inhibitor chloroquine (CQ) or the proteasome inhibitor MG132 to OA3 cells in which knockdown of DNMT3A mutant protein was carried out. The result showed that CQ, but not MG132, reversed CDK1 expression levels, indicating that mutant DNMT3A could up-regulate CDK1 by inhibiting the autophage-lysosome pathway (Fig. 3*E*). Because mTOR is a key negative regulator of autophagy (18), we treated OA3 cells with specific RNAi against mTOR or the mTOR-specific inhibitor rapamycin. Indeed, CDK1 expression decreased with autophagy activation, demonstrated by an increased expression of the autophagy marker LC3-II (Fig. 3 *F* and *G*). Immunofluorescence staining revealed that CDK1 was partly colocalized with LC3. In addition, autophagy activity was further assessed by visualizing a punctate LC3 pattern using confocal microscopy in OA3 cells with knockdown of mutant DNMT3A or treatment with rapamycin (Fig. S3*B*). Notably, both mRNA and protein expression levels of mTOR and its downstream activated proteins, including phosphorylated P70S6K and 4EBP, were considerably higher in NIH 3T3 cells expressing DNMT3A R882H than in cells bearing vehicle or WT DNMT3A (Fig. 3*H*). In agreement with these data in the cell lines, the expression levels of mTOR in BM cells were much higher in Dnmt3a$^{R878H/WT}$ than in Dnmt3a$^{WT/WT}$ mice (Fig. 3*I*).

***Dnmt3a* Mutation Promotes *mTOR* Expression via Hypomethylation.** In view of the gene transcriptional changes of a large number of pathways, including mTOR in BM cells of Dnmt3a$^{R878H/WT}$ mice and the previous finding that DNMT3A mutations could alter DNA methyltransferase activity (2, 10), we hypothesized that the disturbance in genomic methylation might play a role in causing the aberrant transcriptome. Therefore, we performed methylated DNA immunoprecipitation (MeDIP) sequencing for Gr-1$^+$ cells from both Dnmt3a$^{WT/WT}$ and Dnmt3a$^{R878H/WT}$ mice (Dataset S7). Although the number of DNA methylation peaks was not significantly different between the two groups, changes in hypo- and hypermethylation patterns occurred regionally throughout the genome (Fig. S4*A*). We then determined the DNA hypo- and hypermethylation distribution in six regions of gene structure, namely the promoter, downstream of the 3′ UTR, 5′UTR, 3′UTR, coding exon, intron, and intergenic region (Fig. 4*A*). Functional analysis of different methylation regions (DMRs) showed the enrichment of pathways involved in the regulation of the pluripotency of stem cells, MAPK signaling, and CML (Fig. 4*B*). The combination of RNA-seq and MeDIP-seq revealed 145 down-regulated and hypermethylated genes, including *Gata2*, *Gata3*, and *Pax5*, as well as 79 up-regulated and hypomethylated genes, such as *Rpl22*, *Eif4a1*, and *mTOR* (Fig. 4*C* and Dataset S8). Moreover, the MeDIP-seq data of leukemic cells from the same diseased mice showed hypomethylation of the *mTOR* gene in its body region (Fig. 4*D*). These results were consistent with those of a previously established DNMT3A R882H-induced CMML mouse model (Fig. S4*B*). Taken together, our results demonstrated that hypomethylation induced by mutant DNMT3A contributed to mTOR up-regulation, and mTOR overexpression in turn inhibited the autophagy pathway, leading to aberrantly increased CDK1 expression.

Modulation of EZH2 by CDK1 Leads to Changes of H3K27 Trimethylation Enrichment Pattern in Dnmt3a$^{R878H/WT}$ Mice. It was previously reported that CDK1-mediated phosphorylation of EZH2 at threonine 487 could suppress methylation of H3K27 (19, 20). We hypothesized that a similar mechanism could exist in our leukemia model and thus bring another layer of abnormal epigenetic regulation. To explore the possible influence of histone methylation caused by a DNMT3A mutant, we compared the methylation status of histone 3 in BM cells of Dnmt3a$^{WT/WT}$ and Dnmt3a$^{R878H/WT}$ mice. H3K27 trimethylation (H3K27me3) was found decreased whereas H3K4 showed no obvious changes in BM cells of Dnmt3a$^{R878H/WT}$ mice. Meanwhile, EZH2 phosphorylation at threonine (p-EZH2-487) was increased in leukemic BM cells (Fig. 5*A*). We also examined histone 3 methylation patterns in OA3 and 293T cell models. In OA3 cells treated with DNMT3A siRNA, H3K27me3 was increased whereas p-EZH2-487 was decreased compared with cells treated with scrambled siRNA (Fig. 5*B*). In 293T cells transduced with R882H DNMT3A, similar patterns of H3K27 and H3K4 methylation were observed in comparison with control (Fig. S5*A*). These results not only provided evidence that the DNMT3A mutant inhibited H3K27me3 by inducing CDK1-mediated phosphorylation of EZH2 but also encouraged us to evaluate in a systematic way the impact of decreased H3K27me3 on gene expression. We then performed a

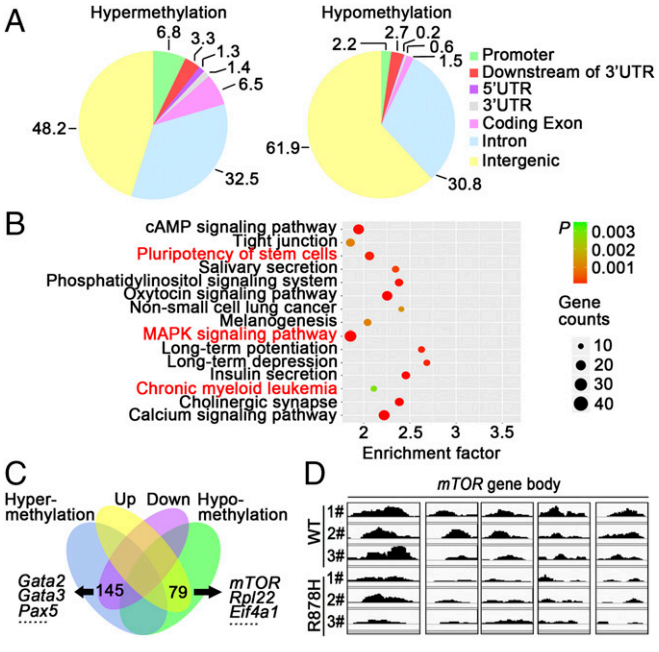

Fig. 4. Dnmt3a mutation promotes mTOR expression via hypomethylation. (*A*) Pie charts showing the average proportions of peaks in each region defined by genomic structure. Peak ratios of hypo- and hypermethylation are shown. (*B*) Functional analysis of DMRs in murine Gr-1$^+$ cells showed a series of enrichments associated with pluripotency of stem cells and CML. (*C*) Venn diagram of the overlapping genes enriched in DMRs and differentially expressed genes. (*D*) MeDIP-seq analysis of the *mTOR* gene showed a local hypomethylation pattern in the gene body in Gr-1$^+$ cells from Dnmt3a$^{R878H/WT}$ mice compared with that of the Dnmt3a$^{WT/WT}$ control.

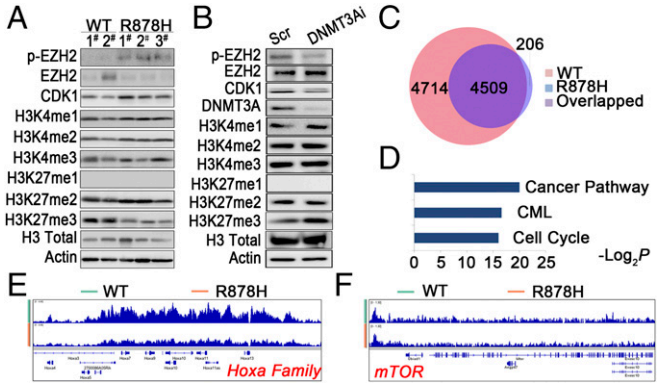

Fig. 5. CDK1-mediated EZH2 phosphorylation resulted in an abnormal H3K27me3 profile. (*A*) Lysates from BM cells of mice were analyzed with Western blot by using the indicated antibodies. (*B*) Lysates from OA3 cells transfected with siRNA against DNMT3A were analyzed with Western blot. (*C*) The number of peaks of H3K27me3 in leukemic cells compared with WT samples. (*D*) KEGG enrichment analysis of genes with loss of enrichment of H3K27me3 in leukemic mice. (*E* and *F*) ChIP-seq profiles of H3K27me3 at the *Hoxa* family genes and *mTOR*.

global ChIP-seq analysis of H3K27me3 on the BM cells of Dnmt3a$^{R882H/WT}$ and Dnmt3a$^{WT/WT}$ mice. The data showed that the peaks of H3K27me3 binding were distributed mainly in the transcription start site regions in both leukemia and WT samples. Notably, the number of genes with enrichment of H3K27me3 was significantly decreased in leukemic cells compared with WT samples (Fig. 5*C*). Among the genes with reduced H3K27me3 enrichment levels, those related to pathways such as "cancer," "CML," and "cell cycle" drew our attention (Fig. 5*D*). For example, the *Hoxa* family was found to have decreased enrichment of H3K27me3, in concordance with the transcriptional activation of several *Hoxa* genes (Fig. 5*E*). However, there was no major change of H3K27me3 status in the *mTOR* gene (Fig. 5*F*). Hence, mTOR activation could more likely be caused by decreased DNA methylation (Fig. 4*D*).

Rapamycin Inhibits Proliferation of Human *DNMT3A* Mutation-Related Leukemia Cell Lines and Leukemic Cells in Dnmt3a$^{R878H/WT}$ Mice. In an attempt to identify potential therapeutic agents against leukemia associated with *DNMT3A* mutations, we found a relatively specific inhibition of the proliferation of OA3 and OCI-AML2 (OA2) cells by rapamycin (Fig. 6*A*). We then performed a colony-formation assay and morphological analysis of leukemic cells with or without the *DNMT3A* mutation in the presence of rapamycin for 2 wk. The number of colonies carrying the *DNMT3A* mutation significantly decreased after treatment with rapamycin (Fig. 6*B*), whereas no changes of surface marker expression were found in OA3 colony cells (Fig. S6*A*). To determine the reason behind the high sensitivity of cells carrying the *DNMT3A* mutation to rapamycin, we examined the expression of mTOR in different subtypes of AML cell lines. OA2 and OA3 cells exhibited a higher mTOR expression than cells with WT DNMT3A (Fig. 6*C*). We further determined the in vivo effect of rapamycin (4 mg/kg for 4 mo) on BM cells in Dnmt3a$^{R878H/WT}$ mice. Indeed, the compound significantly reduced the percentage of immature cells in the BM (Fig. 6*D* and Fig. S6*B*) and the leukemic cell infiltration in the spleen (Fig. 6*E* and Fig. S6*C*). mTOR has been recently reported to play a role in adaptive transition of quiescent stem cells from G_0 to G_{Alert} (21). Similarly, the percentage and number of both LSK and LRP cells significantly decreased in Dnmt3a$^{R878H/WT}$ mice treated with rapamycin (Fig. 6*F* and Fig. S6*D*). Upon treatment with rapamycin, survival of Dnmt3a$^{R878H/WT}$ mice significantly improved compared with controls (Fig. 6*G*). Furthermore, we also examined fresh BM samples of AML patients. RT-PCR and Western blot analysis demonstrated that samples carrying DNMT3A R882H exhibited a higher expression of mTOR than those with WT DNMT3A (Fig. S6 *E* and *F*). These results suggested that rapamycin inhibits proliferation of leukemic cells carrying the *DNMT3A* mutation.

Discussion

The importance of *DNMT3A* in hematopoiesis and leukemogenesis has been demonstrated by studies using *Dnmt3a* knockout or DNMT3A R882-overexpressing mice (7, 12, 22). In this study, the conditional knockin mouse model allowed the inducible allelic switch from Dnmt3a$^{WT/WT}$ to Dnmt3a$^{R878H/WT}$ in the hematopoietic system of adult animals, which indeed possessed some major features of human AML associated with the *DNMT3A* mutation. This strategy bypassed the embryonic lethality associated with *Dnmt3a* R878H expression, thus providing a relevant model for studying the target genes regulated by *Dnmt3a* R878H. Our data therefore highlight the crucial roles of endogenous expression of mutant Dnmt3a R878H in malignant hematopoiesis. Considering that most of the reported *DNMT3A* mutations in human myeloid neoplasms are heterozygous (1, 2), we observed a transplantable AML phenotype in Dnmt3a$^{R878H/WT}$ heterozygous animals whereas homozygous mice showed growth inhibition and died soon after birth. The leukemia phenotype in mice bore some similarities to that in a *Dnmt3a*$^{-/-}$ murine model (23). Our results showed that leukemic LSKs were composed mostly of LRPs and contained leukemia-initiating cells. These data indicated that *Dnmt3a* mutation could promote proliferation of leukemic stem/progenitor cells by accelerating the transition of HSPCs from a quiescent status to an active one. However, it was just reported that a knockin of the same allele did not cause leukemia on its own with a 2-y follow-up (24). The generation of distinct phenotypes might be caused by different conditional knockin design, mice strain, and so forth. Moreover, we found that differentiation of erythroid progenitors was arrested, consistent with previous reports (25).

In AML patients studied with exome sequencing, 4 out of 51 cases had the *DNMT3A* mutation as the only known abnormal genetic event (26). In our Dnmt3a$^{R878H/WT}$ mice, exome sequencing and RNA-seq revealed the *Dnmt3a* mutation in leukemic cells without recurrent mutations of genes that are well-known coexisting events in human AML with a *DNMT3A* abnormality. It is worth noting that our leukemia model is a relatively moderate one, because the disease developed after a relatively long latency period (4 to 6 mo) and displayed a quite lengthy median survival

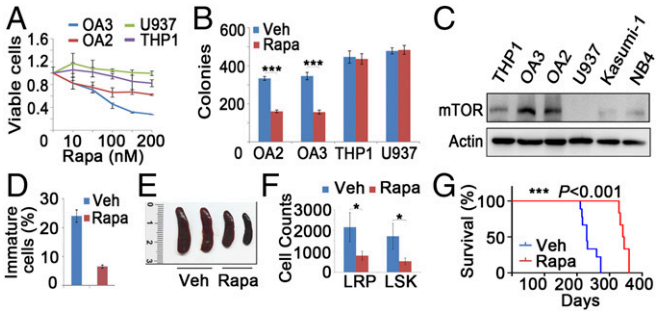

Fig. 6. Rapamycin inhibits the proliferation of Dnmt3a$^{R878H/WT}$ and human DNMT3A mutated leukemic cells. (*A*) Response of OA3, OA2, THP1, and U937 cells to rapamycin (rapa). (*B*) Colony-formation assay of AML-related cells treated with rapamycin for 2 wk. Veh, vehicle. (*C*) Lysates of cells from different AML subtypes were analyzed with Western blot. (*D*) Statistical analysis of the number of immature cells in the BM treated with veh or rapa for 4 mo. (*E*) Macroscopic appearance of the spleen from Dnmt3a$^{R878H/WT}$ mice treated with veh or rapa for 4 mo. (*F*) Numbers of LSKs and LRPs in Dnmt3a$^{R878H/WT}$ mice treated with veh or rapa for 4 mo. (*G*) Kaplan–Meier survival analysis of Dnmt3a$^{R878H/WT}$ mice treated with veh ($n = 8$) or rapa ($n = 6$) (4 mg/kg) for 4 mo. Mean ± SEM values are shown. $^*P < 0.05$, $^{***}P < 0.001$.

time (230 d), and the average percentage of immature cells in the BM was only 23%. Hence, although our model proved the leukemogenic effect of the *DNMT3A* mutation, it may provide tools to study the role of cooperating mutations for a more aggressive full-blown AML to occur.

In the mechanism study, our *Dnmt3a* R878H mice have shown that leukemic cells have altered gene expression and epigenetic regulatory patterns contributing to the growth/survival advantage over WT mice. Single-cell RNA-seq of LSKs revealed that the gene expression heterogeneity in leukemic samples seemed to be higher than in WT controls. This, together with the significantly increased number of LSKs/LRPs in Dnmt3a$^{R878H/WT}$ mice, could underlie the clonal diversity and evolutionary potential of leukemia-initiating cells along with the disease course. Moreover, we found that clusters of genes, such as *Hoxa* family, cell-cycle, and mTOR signal pathways, which are activated in leukemic progression, were overexpressed. A recent study shed light on Dnmt3b having synergistic effects with Dnmt3a in leukemogenesis, which might contribute to the coexistence of hyper- and hypomethylated genes in Dnmt3a$^{R878H/WT}$ cells (27). These data have not only confirmed but also largely extended the knowledge that we previously acquired from samples obtained from AML patients.

The *DNMT3A* R882H mutation enhances expression of CDK1, which facilitates transition of hematopoietic cells to the S/G_2/M phase. mTORC1 activity is necessary and sufficient for the transition of stem cells from a quiescent status to an active one (21). The present study found that the *DNMT3A* mutation contributed to hypomethylation in the gene body region of *mTOR* in Dnmt3a$^{R878H/WT}$ mice. The resultant overexpression of mTOR inhibited the autophage pathway and finally led to an aberrantly high level of CDK1. CDK1 phosphorylated EZH2 at T487, attenuated the ability of this enzyme to catalyze trimethylation of H3K27, and possibly influenced an array of genes associated with leukemic progression such as the *Hoxa* family.

Finally, our in vitro and in vivo data indicated a potential antitumor activity of the mTOR inhibitor in DNMT3A-mutated leukemia. AML cell lines with the *DNMT3A* mutation were responsive to rapamycin treatment, and the differential sensitivity displayed may be determined by the expression levels of mTOR. Consistent with in vitro results, our findings revealed that rapamycin elicited a therapeutic response in Dnmt3a$^{R878H/WT}$ mice. Hence, we would like to suggest that further possible preclinical and clinical studies of mTOR inhibitors be carried out in AML-M5 and -M4 subtypes with *DNMT3A* mutations.

Materials and Methods

Generation of Dnmt3a$^{R878H/WT}$ Mx1Cre^{+} Mice and Breeding. Dnmt3a$^{R878H/WT}$ mice were obtained from the Nanjing Biomedical Research Institute of Nanjing University. Targeting vectors PL253 used to establish Dnmt3a R878H conditional knockin mice were generated through recombineering (Fig. S1*A*). Subsequent genotyping of offspring was performed by PCR analysis with primers specific for the Dnmt3a R878H mutation (Datasets S9 and S10). To activate transgene expression in vivo, we administered pIpC to the animals at the time of weaning (4 wk old). Details of treatment protocols are available in *SI Materials and Methods*. Mice were used according to animal care standards, and all protocols were approved by the Committee on Animal Use for Research at the Shanghai Jiao Tong University School of Medicine.

cDNA Library Preparation from Single Cells Using Fluidigm C1. For each culture condition, 3,000 to 4,000 sorted LSKs were loaded onto a 10- to 17-mm Fluidigm C1 Single-Cell Auto Prep Integrated Fluidic Circuit (IFC), and cells were captured according to the manufacturer's instructions. Libraries from one chip were pooled, and paired-end 200-bp sequencing was performed on four lanes of an Illumina MiSeq. We sequenced an average of over 4.4 million reads per cell (details are in *SI Materials and Methods*).

Treatment of Dnmt3a$^{R878H/WT}$ Mice with Rapamycin. Five weeks after the birth of induced Dnmt3a$^{R878H/WT}$ mice, they were subjected to the following treatment protocols: normal saline (vehicle) or rapamycin administered at 4 mg/kg twice a wk for 4 wk, followed by the administration of the same dose once per wk for 4 mo.

The other procedures, including Western blot, flow cytometric analysis, RNA-seq, and MeDIP-seq, are described in *SI Materials and Methods*. All patients gave informed consent for research use. The research involving humans was approved by the institutional review board of Rui Jin Hospital.

ACKNOWLEDGMENTS. We thank all of our colleagues at the Shanghai Institute of Hematology for constructive discussions and technical help. This work was supported by the National Key Basic Research Program of China (2013CB966800), Ministry of Health Grant 201202003, Mega-Projects of Scientific Research for the 12th Five-Year Plan (2013ZX09303302), National Natural Science Foundation of China (81123005, 81222004, and 81570151), Samuel Waxman Cancer Research Foundation, Shanghai Talent Development Fund 201458, Shanghai Municipal Education Commission-Gaofeng Clinical Medicine Grant 20152507, Center for HPC Shanghai Jiao Tong University, and Innovation Foundation for Doctoral Students of Shanghai Jiao Tong University School of Medicine Grant BXJ201611.

1. Ley TJ, et al. (2010) DNMT3A mutations in acute myeloid leukemia. *N Engl J Med* 363: 2424–2433.
2. Yan XJ, et al. (2011) Exome sequencing identifies somatic mutations of DNA methyltransferase gene DNMT3A in acute monocytic leukemia. *Nat Genet* 43:309–315.
3. Walter MJ, et al. (2011) Recurrent DNMT3A mutations in patients with myelodysplastic syndromes. *Leukemia* 25:1153–1158.
4. Neumann M, et al. (2013) Whole-exome sequencing in adult ETP-ALL reveals a high rate of DNMT3A mutations. *Blood* 121:4749–4752.
5. Shen Y, et al. (2011) Gene mutation patterns and their prognostic impact in a cohort of 1185 patients with acute myeloid leukemia. *Blood* 118:5593–5603.
6. Thol F, et al. (2011) Incidence and prognostic influence of DNMT3A mutations in acute myeloid leukemia. *J Clin Oncol* 29:2889–2896.
7. Challen GA, et al. (2011) Dnmt3a is essential for hematopoietic stem cell differentiation. *Nat Genet* 44:23–31.
8. Shlush LI, et al.; HALT Pan-Leukemia Gene Panel Consortium (2014) Identification of pre-leukaemic haematopoietic stem cells in acute leukaemia. *Nature* 506:328–333.
9. Kim SJ, et al. (2013) A DNMT3A mutation common in AML exhibits dominant-negative effects in murine ES cells. *Blood* 122:4086–4089.
10. Russler-Germain DA, et al. (2014) The R882H DNMT3A mutation associated with AML dominantly inhibits wild-type DNMT3A by blocking its ability to form active tetramers. *Cancer Cell* 25:442–454.
11. Neri F, et al. (2013) Dnmt3L antagonizes DNA methylation at bivalent promoters and favors DNA methylation at gene bodies in ESCs. *Cell* 155:121–134.
12. Xu J, et al. (2014) DNMT3A Arg882 mutation drives chronic myelomonocytic leukemia through disturbing gene expression/DNA methylation in hematopoietic cells. *Proc Natl Acad Sci USA* 111:2620–2625.
13. Yang X, et al. (2014) Gene body methylation can alter gene expression and is a therapeutic target in cancer. *Cancer Cell* 26:577–590.
14. Celik H, et al. (2015) Enforced differentiation of Dnmt3a-null bone marrow leads to failure with c-Kit mutations driving leukemic transformation. *Blood* 125:619–628.
15. Mayle A, et al. (2015) Dnmt3a loss predisposes murine hematopoietic stem cells to malignant transformation. *Blood* 125:629–638.
16. Kiel MJ, et al. (2005) SLAM family receptors distinguish hematopoietic stem and progenitor cells and reveal endothelial niches for stem cells. *Cell* 121:1109–1121.
17. Kolodziejczyk AA, et al. (2015) Single cell RNA-sequencing of pluripotent states unlocks modular transcriptional variation. *Cell Stem Cell* 17:471–485.
18. Adams J (2004) The proteasome: A suitable antineoplastic target. *Nat Rev Cancer* 4:349–360.
19. Wei Y, et al. (2011) CDK1-dependent phosphorylation of EZH2 suppresses methylation of H3K27 and promotes osteogenic differentiation of human mesenchymal stem cells. *Nat Cell Biol* 13:87–94.
20. Wu SC, Zhang Y (2011) Cyclin-dependent kinase 1 (CDK1)-mediated phosphorylation of enhancer of zeste 2 (Ezh2) regulates its stability. *J Biol Chem* 286:28511–28519.
21. Rodgers JT, et al. (2014) mTORC1 controls the adaptive transition of quiescent stem cells from G0 to G(Alert). *Nature* 510:393–396.
22. Yang L, et al. (2016) DNMT3A loss drives enhancer hypomethylation in FLT3-ITD-associated leukemias. *Cancer Cell* 29:922–934.
23. Guryanova OA, et al. (2016) Dnmt3a regulates myeloproliferation and liver-specific expansion of hematopoietic stem and progenitor cells. *Leukemia* 30:1133–1142.
24. Guryanova OA, et al. (2016) DNMT3A mutations promote anthracycline resistance in acute myeloid leukemia via impaired nucleosome remodeling. *Nat Med* 22:1488–1495.
25. Zhang X, et al. (2016) DNMT3A and TET2 compete and cooperate to repress lineage-specific transcription factors in hematopoietic stem cells. *Nat Genet* 48:1014–1023.
26. Ley TJ, et al.; Cancer Genome Atlas Research Network (2013) Genomic and epigenomic landscapes of adult de novo acute myeloid leukemia. *N Engl J Med* 368:2059–2074.
27. Zheng Y, et al. (2016) Loss of Dnmt3b accelerates MLL-AF9 leukemia progression. *Leukemia* 30:2373–2384.
28. Wen ZH, et al. (2013) Critical role of arachidonic acid-activated mTOR signaling in breast carcinogenesis and angiogenesis. *Oncogene* 32:160–170.
29. Kim DH, et al. (2002) mTOR interacts with raptor to form a nutrient-sensitive complex that signals to the cell growth machinery. *Cell* 110:163–175.
30. Iwamaru A, et al. (2007) Silencing mammalian target of rapamycin signaling by small interfering RNA enhances rapamycin-induced autophagy in malignant glioma cells. *Oncogene* 26:1840–1851.